Kinetic and Mechanistic Studies of the Electrocatalytic Reduction of O₂ to H₂O with Mononuclear Cu Complexes of Substituted 1,10-Phenanthrolines[†]

Charles C. L. McCrory, Xavier Ottenwaelder,[‡] T. Daniel P. Stack, and Christopher E. D. Chidsey*

Department of Chemistry, Stanford University, Stanford, California 94305

Received: July 31, 2007; In Final Form: August 27, 2007

Mononuclear Cu complexes with a 1,10-phenanthroline-based ligand adsorbed onto an edge-plane graphite electrode act as electrocatalysts for the 4-electron reduction of O₂ to H₂O. A mechanism is proposed for the electrocatalytic O₂ reduction that accounts for the observed redox and kinetic dependences on coordinating anions and proton donors in the buffer. Systematic increases of ligand electron-withdrawing properties and/ or the steric demands near the Cu center increase the E^0 of the Cu catalysts but decrease the rate of O₂ reduction. The kinetic rate of O₂ reduction at E^0, reported as kinetic current divided by catalyst redox charge, decreases as E^0 increases: from 16 s^{-1} measured at E^0 in air-saturated solutions for adsorbed Cu(phen) to 0.4 s^{-1} for Cu(2,9-Et₂-phen). The maximum value of E for which catalytic activity can be attained is estimated to be +350 mV vs NHE. Near E^0, the kinetic current deviates from that expected if O₂ binding were the sole rate-limiting step. This indicates that one or more of the electrochemical reduction steps are rate limiting at potentials near E^0.

Introduction

Molecular Cu catalysts may be viable alternatives to nanoparticulate Pt catalysts for the 4-electron reduction of O₂ to H₂O in low-temperature fuel cells and related devices. This is evidenced by the Cu-containing fungal laccase enzymes that reduce O₂ directly to water at a trinuclear Cu active site at remarkably positive potentials.[1,2] High current densities of ca. 5 mA/cm² at overpotentials of only −70 mV from the thermodynamic potential of O₂ reduction have been reported recently by Heller and colleagues with specially designed laccase-modified electrodes at pH 5.[3-5] This current density corresponds to a turnover rate of 2.1 O₂ reduced per laccase s^{-1}, or 0.7 O₂ per Cu s^{-1}. In contrast, Pt nanoparticulate catalysts reduce O₂ with rates of 2.5 O₂ per active surface Pt s^{-1}, or 0.25 O₂ per total Pt s^{-1}, at a much less attractive overpotential of −350 mV.[6] Normalizing these rates per metal atom allows for direct comparison of both the atom efficiency and kinetic rate of O₂ reduction regardless of catalyst loading.

Synthetic Cu complexes provide a degree of flexibility not available in enzymatic systems and can help define the minimal ligand set that, when complexed with Cu, can promote O₂ reduction at low overpotentials and high current densities. Here we consider a family of mononuclear Cu complexes for O₂ reduction. Although mononuclear Cu complexes are unlikely to achieve high turnover rates at overpotentials as attractive as those of multinuclear systems, they constitute an appropriate starting point to define the catalytic limitations of Cu-based molecular catalysts before developing more elaborate constructs.

Anson and co-workers discovered that the oxidatively robust 1,10-phenanthroline (phen) complexes of Cu, when adsorbed onto edge-plane graphite, catalyze the 4-electron reduction of O₂ to H₂O.[7-10] The resulting adsorbed complexes were assigned to be 1:1 complexes of the phen-based ligand to Cu.[7-10] A mechanism was proposed for the electrocatalytic 4-electron reduction of O₂ and the associated rate constants were determined.[7,10] Using three phen-based complexes (phen, 2,9-Me₂-phen, 5-Cl-phen), it was shown that the reduction of O₂ occurs negative of the Cu$^{II/I}$ redox potential and that the rate constant of O₂ reduction measured at very negative potential decreases as the Cu$^{II/I}$ redox potential increases toward the thermodynamic potential of O₂ reduction (940 mV vs NHE at pH 4.8).[7] These studies were conducted in a broad-range buffer system containing acetate, phosphate, and borate. However, the proposed mechanism did not include coordination of these anions, even though these anions are known to alter the potentials and electrocatalytic behavior of similar complexes.[11]

Our study sought to better understand the O₂-reduction mechanism for phen-based Cu complexes, including the influence of coordinating anions and of specific acids in solution. We have prepared a library of phen-based ligands and studied their Cu complexes adsorbed on edge-plane graphite electrodes for electrocatalytic reduction of O₂. We have specifically examined how the rate of electrocatalysis *at the redox potential of the catalyst* changes as the redox potential increases due to variation of the phen-based ligand. We find a much more abrupt drop in O₂-reduction activity measured at the redox potential of the Cu catalyst than that measured at very negative potential (and thus high overpotential). We discuss the implications of this finding on the mechanism of the electrocatalytic reduction of O₂ by mononuclear Cu catalysts and estimate the most positive potential at which these catalysts are likely to function.

Experimental Section

Ligands. Phen (1,10-phenanthroline), 5-Cl-phen, 5-NO₂-phen, 2,9-Me₂-phen, and 2,9-*n*Bu₂-phen were obtained from commercial sources. 2,9-*n*Bu₂-phen was further purified by chro-
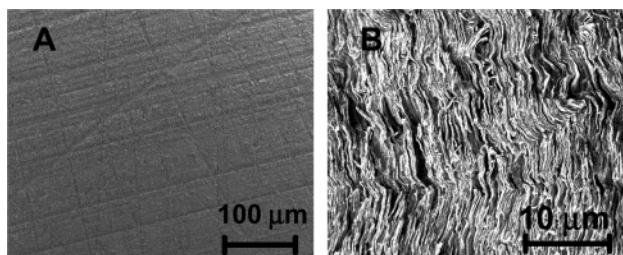
Figure 1. Scanning electron micrographs of the EPG surface at a magnification of (a) 650x and (b) 10000x. The higher magnification shows a structure with deep, micron-sized crevices that can accommodate ligand adsorption into the electrode.

matography over silica with dichloromethane saturated with wet ammonia as the eluent. 2-Me-phen,[12] 5-NH$_2$-phen,[13] and 5-NO$_2$-2,9-Me$_2$-phen[14,15] were prepared according to literature procedures. 2,9-Et$_2$-phen was prepared by adapting a literature procedure with commercial ethyl lithium.[16] 3,8-(CO$_2$Et)$_2$-4,7-Cl$_2$-phen was prepared similarly to 3-CO$_2$Et-4-Cl-phen,[17] by deoxychlorination of 1,4,7,10-tetrahydro-3,8-dicarboethoxy-1,-10-phenanthroline-4,7-dione.[18,19] 5-NH$_2$-2,9-Me$_2$-phen[20] was prepared by the reduction of 5-NO$_2$-2,9-Me$_2$-phen in a manner similar to 5-NH$_2$-phen.[13] Purification of 2-Me-phen, and 2,9-Et$_2$-phen was possible by chromatography over silica with dichloromethane saturated with wet ammonia as the eluent. This eluent yields well-separated TLC spots with no tailing effects and has proven extremely useful in the purification of phen derivatives. The purity of all compounds was assessed by solution ^{1}H NMR on a Varian Innova 300 MHz instrument.

Apparatus and Procedures. Edge-plane graphite (EPG) disk electrodes with a 0.195 cm^2 macroscopic surface area purchased from Pine Instrument Company were used unless otherwise specified. The electrodes were ground by hand with a 600-grit SiC paper followed by sonication in pure water before each ligand deposition. As seen by scanning electron microscopy, the resulting EPG surfaces have mica-like leafy forms perpendicular to the grinding plane (Figure 1), which increase the surface area of the electrode and presumably allow intercalation of the complexes between graphene sheets. Ligands were adsorbed onto the electrode surface either by exposing the surface to 1 mM aqueous solutions of the ligand made by addition of appropriate amounts of saturated solutions of the ligand in acetonitrile to water (final solution less than 10% acetonitrile by volume) or by depositing a known quantity of the ligand dissolved in 1,1,1-trichloroethane and subsequent evaporation of the solvent. Cu^{II} was incorporated by exposing the electrodes to 500 mM aqueous solutions of Cu(NO$_3$)$_2$ and then rinsing with water. Electrochemical measurements were recorded with a Pine Instrument Company AFCBP1 bipotentiostat with a MSR rotator, an auxiliary Pt-mesh electrode and a Ag/AgCl/NaCl(sat) reference electrode. The reference was calibrated against Cu(NO$_3$)$_2$ in 1 M KBr,[21] and all reported values are referenced to NHE.

Results

Anion Dependence. The complex formed by adsorbing 2,9-Me$_2$-phen onto an edge-plane graphite (EPG) electrode and then exposing the electrode to aqueous Cu(NO$_3$)$_2$ was investigated in depth as a specific example of the complexes formed between various phen-based ligands and Cu on EPG. We denote this complex as Cu(2,9-Me$_2$-phen). Cyclic voltammograms (CVs) of Cu(2,9-Me$_2$-phen) in contact with a Cu-free electrolyte under a N$_2$ atmosphere (Figure 2) show reversible reduction and oxidation peaks with full-widths-at-half-maximum of ca. 120
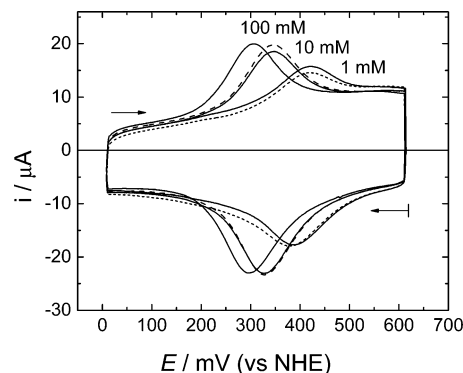

Figure 2. Cyclic voltammograms of Cu(2,9-Me$_2$-phen) adsorbed onto an EPG electrode in N$_2$-purged 100 mM NaClO$_4$(aq) buffered with equal concentrations of NaAcO and AcOH to pH 4.8 (scan rate 100 mV/s). The sum of [AcO$^-$] and [AcOH] was increased (—) from 1 to 100 mM and then decreased (---) from 100 mM back to 1 mM.
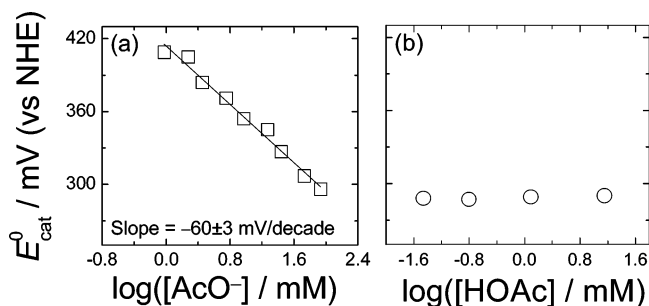

Figure 3. (a) $E^0_{cat.}$ plotted against log([AcO$^-$]/mM) in 100 mM NaClO$_4$(aq) with no AcOH added to the solution. (b) $E^0_{cat.}$ plotted against log([AcOH]/mM) in 1 M NaClO$_4$ and 100 mM NaAcO.

mV and a separation of the reduction and oxidation peak potentials of ca. 20 mV at a scan rate of 100 mV/s. These features are assigned to the Cu$^{II/I}$ redox couple.[7,10] The standard redox potential of the complex, $E^0_{cat.}$, is taken to be the average of the peak potentials. A plot of the peak current as a function of scan rate is linear (see Supporting Information), confirming that the electroactive complex is surface adsorbed. Increasing the concentration of the acetate buffer in the electrolyte by 2 orders of magnitude from 1 to 100 mM both increases the peak current and decreases $E^0_{cat.}$. These effects are reversible: decreasing the acetate buffer concentration decreases the peak current and increases $E^0_{cat.}$ (Figure 2).

The effects of the acetate concentration, [AcO$^-$], and the acetic acid concentration, [AcOH], on $E^0_{cat.}$ are more clearly illustrated in Figure 3. Increasing [AcO$^-$] in the absence of added AcOH decreases $E^0_{cat.}$. The plot of $E^0_{cat.}$ versus log-([AcO$^-$]/mM) is linear with a slope of −60 mV/decade of [AcO$^-$] (Figure 3a). At constant [AcO$^-$], varying [AcOH] does not change $E^0_{cat.}$ (Figure 3b). These effects clearly demonstrate a dependence of $E^0_{cat.}$ on [AcO$^-$], but no dependence on [AcOH], and therefore no dependence on pH.

The peak current also changes reversibly with changing [AcO$^-$] and is independent of [AcOH]. The increase of peak current observed in Figure 2 as [AcO$^-$] is increased cannot be due to adsorption of additional Cu or 2,9-Me$_2$-phen because neither is present in the electrolyte. The amount of Cu complex on the surface is therefore conserved, but the amount that is electrochemically active varies. This somewhat surprising result motivated further study of the fraction of the adsorbed complex that is electrochemically active as a function of the surface coverage of 2,9-Me$_2$-phen and as a function of [AcO$^-$] in the electrolyte.
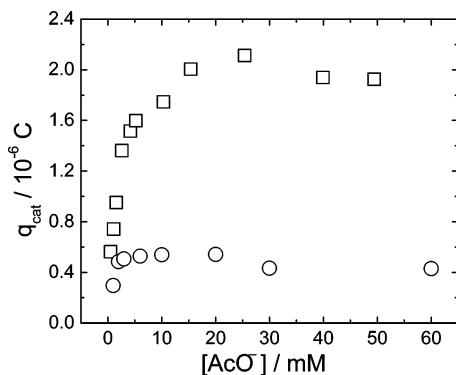
Electrocatalytic Reduction of O$_2$ to H$_2$O

J. Phys. Chem. A, Vol. 111, No. 49, 2007 **12643**

Figure 4. $q_{cat.}$ as a function of [AcO$^-$] (squares) at a high 2,9-Me$_2$-phen coverage of 9×10^{-10} mol/cm^2 and (circles) at a low 2,9-Me$_2$-phen coverage of 2×10^{-10} mol/cm^2. Cu was incorporated from 500 mM Cu(NO$_3$)$_2$(aq).

The redox charge associated with the Cu$^{II/I}$ interconversion, $q_{cat.}$, is a direct measure of the amount of complex that is electroactive. It is measured from an integration of the area of the Cu$^{II/I}$ redox peak in the CV.[22] A plot of $q_{cat.}$ vs [AcO$^-$] is shown in Figure 4. Electrodes with both a high (9×10^{-10} mol/cm^2) and a low (2×10^{-10} mol/cm^2) coverage of 2,9-Me$_2$-phen were prepared by evaporating solutions of known ligand concentration onto the surface. The ligands then were complexed with Cu by exposing the electrodes to 500 mM Cu(NO$_3$)$_2$(aq). The $q_{cat.}$ measurements were taken in Cu-free electrolyte solutions. In the cases of both high and low coverage, charge plateaus are observed as a function of [AcO$^-$], but the plateau is reached at lower [AcO$^-$] in the lower coverage case: [AcO$^-$] = 2 mM at low coverage vs [AcO$^-$] = 15 mM at high coverage. In either case, the measured charge at the plateau represents ca. 30% of the expected charge if all the deposited 2,9-Me$_2$-phen binds Cu and is electroactive.

Cu(2,9-Me$_2$-phen) shows a similar potential and charge dependence on the concentrations of some anions other than AcO$^-$. CVs with bicarbonate and carbonate buffers are shown in Figure 5a,b, respectively. Upon increasing either the carbonate or bicarbonate ion concentrations, $E_{cat.}^0$ decreases by approximately −60 mV/decade and the peak currents increase. Analogous experiments with more weakly coordinating anions such as perchlorate or nitrate do not show these concentration dependences.

Exposing the surface to Cu(ClO$_4$)$_2$(aq) and CuCl$_2$(aq) does not change the measured charge appreciably. However, complexing the ligand with Cu by exposing the electrode to aqueous solutions of Cu(NO$_3$)$_2$ and a high concentration of NaAcO leads to increases in the measured charge. For instance, with a high 2,9-Me$_2$-phen coverage of 9×10^{-10} mol/cm^2, the charge increases from $4.2 \pm 0.3 \times 10^{-6}$ C for electrodes exposed to 500 mM Cu(NO$_3$)$_2$ and 10 mM NaAcO to $8.0 \pm 0.6 \times 10^{-6}$ C for electrodes exposed to 500 mM Cu(NO$_3$)$_2$ and 1 M NaAcO (measurements made in a Cu-free electrolyte with [AcO$^-$] = 5 mM).

O$_2$ Reduction. In air-saturated solutions, we observe a current attributed to catalytic O$_2$ reduction. The solid line in Figure 6a is the CV of an EPG electrode with adsorbed Cu(2,9-Me$_2$-phen) in an air-saturated aqueous solution of 20 mM NaAcO and 100 mM NaClO$_4$. The dashed line is the CV of the surface-adsorbed complex in the same solution purged with N$_2$(g); $E_{cat.}^0$ is +310 mV vs NHE. The current in the negative-going scan in the air-saturated voltammogram is comparable to that of the N$_2$-purged voltammogram until the potential decreases below ca. 300 mV vs NHE, at which point the current increases abruptly. This increase is attributed to the electrocatalytic reduction of O$_2$ in the air-saturated solution. Addition of [AcOH] = 0.4 mM
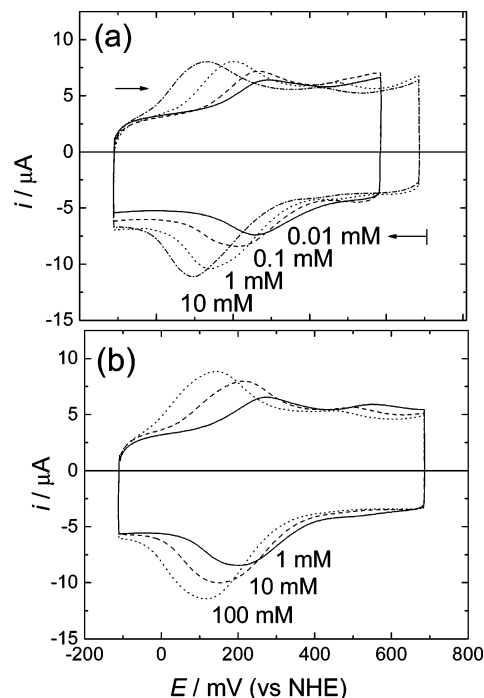

Figure 5. Cu(2,9-Me$_2$-phen) adsorbed onto EPG in varying concentrations of (a) Na$_2$CO$_3$ (measured pH = 10.2) and (b) NaHCO$_3$ (measured pH = 7.5) (100 mV/s; 100 mM NaClO$_4$).

(Figure 6b) enhances the current of the peak near the Cu$^{II/I}$ reduction potential and moderately reduces the current of the peak at 160 mV vs NHE. At higher [AcOH] (Figure 6c), only the peak near the Cu$^{II/I}$ redox potential is evident. In summary, the Cu complex is electrocatalytic at $E_{cat.}^0$ in the presence of AcOH but at low [AcOH] is electrocatalytic only at more negative potentials. This suggests that AcOH plays a key role in the O$_2$-reduction mechanism and indicates that there is a rate-limiting electron-transfer step negative of $E_{cat.}^0$ for solutions with limited [AcOH].

AcOH also appears to prevent irreversible changes to the complex during O$_2$ reduction. In the absence of added AcOH, if the electrode potential is held at −200 mV vs NHE with a constant rate of O$_2$ delivery to the electrode,[23] dramatic and irreversible changes are found over time (Figure 7). After 300 s, a reversible peak is obtained at 20 mV vs NHE (measured in an N$_2$-purged solution) with a corresponding decrease of the peak at 310 mV vs NHE (Figure 7a). After 1080 s, the peak at +310 mV vs NHE is almost fully replaced by the peak at 20 mV vs NHE (Figure 7b). Stripping the Cu from the ligand by exposing the surface to [AcOH] = 1.0 M, followed by Cu reloading with 50 mM Cu(NO$_3$)$_2$, provides a CV similar to Figure 7b. This indicates that the change is due to an irreversible modification of the ligand. No ligand modification is observed with [AcOH] > 2 mM.

Ligand Dependence. For the studies of the ligand dependence, a 20 mM NaAcO and 20 mM AcOH buffer (pH 4.8) was used, which ensures both adequate [AcO$^-$] to give a well-defined Cu^{II}/Cu^I redox peak and adequate [AcOH] to promote O$_2$ reduction near the standard redox potential of the complex, $E_{cat.}^0$ (cf. Figure 6c), while also preventing irreversible ligand modification.

Figure 8 shows representative CVs for Cu complexes of four ligands investigated: phen, 3,8-(CO$_2$Et)$_2$-4,7-Cl$_2$-phen, 2,9-Me$_2$-phen, and 5-NO$_2$-2,9-Me$_2$-phen. 3,8-(CO$_2$Et)$_2$-4,7-Cl$_2$-phen (Fig-

12644 *J. Phys. Chem. A, Vol. 111, No. 49, 2007*

McCrory et al.

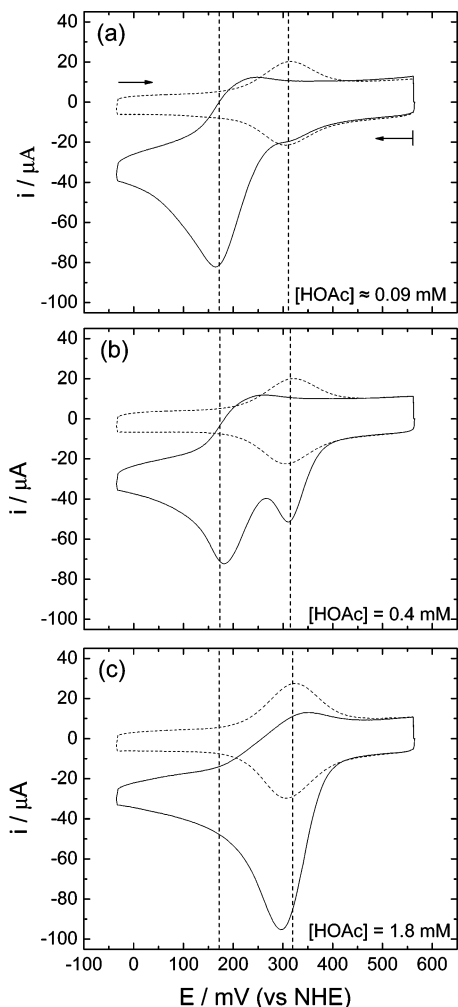**Figure 6.** Electrocatalytic reduction of O_2 by Cu(2,9-Me$_2$-phen) adsorbed onto EPG in N$_2$-purged (---) and air-saturated (—) solutions of 100 mM NaClO$_4$, 20 mM NaAcO with different concentrations of AcOH at 100 mV/s. The increase in the current in the air-saturated solution is indicative of the electrocatalytic reduction of O_2. (a) With no added AcOH, one O_2-reduction peak is observed, centered at ca. 160 mV. (The calculated [AcOH] for this solution due to acid dissociation is 0.09 mM.) (b) With [AcOH] = 0.4 mM another O_2-reduction peak appears near $E_{cat.}^0$. (c) With [AcOH] = 1.8 mM, only the peak near $E_{cat.}^0$ is evident.

ure 8b) shifts both $E_{cat.}^0$ and the potential of the O_2-reduction peak, E_{O_2}, positive with respect to those of phen (Figure 8a). 2,9-Me$_2$-phen (Figure 8c) shifts $E_{cat.}^0$ and E_{O_2} more positive with respect to phen. 2,9-Me$_2$-5-NO$_2$-phen (Figure 8d) shifts $E_{cat.}^0$ even more positive, but E_{O_2} occurs at a significantly more negative potential than for 2,9-Me$_2$-phen or 3,8-(CO$_2$Et)$_2$-4,7-Cl$_2$-phen.

$E_{cat.}^0$ and E_{O_2} are tabulated for a broader set of ligands in Table 1; data on additional ligands are reported in the Supporting Information. Three trends are evident for the ligands reported in Table 1. First, $E_{cat.}^0$ increases as electron-withdrawing substituents are added to the ligand at positions remote to the Cu-binding site. For example, $E_{cat.}^0$ of Cu(3,8-(CO$_2$Et)$_2$-4,7-Cl$_2$-phen) is 60 mV more positive than that of Cu(3-CO$_2$Et-4-Cl-phen) and 125 mV more positive than Cu(phen). Second, $E_{cat.}^0$ increases as the steric demands of the substituents in the 2 and 9 positions adjacent to the Cu-binding site increase. For example, $E_{cat.}^0$ of Cu(2,9-Me$_2$-phen) is 95 mV more positive than that of Cu(2-Me-phen), and 290 mV more positive than that of Cu-(phen). These two effects can be combined. Cu(2,9-Me$_2$-5-NO$_2$-
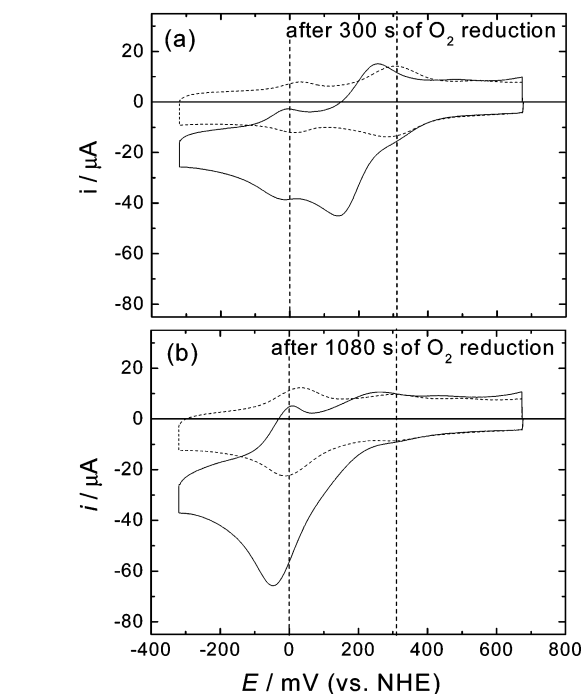

Figure 7. Cu(2,9-Me$_2$-phen) adsorbed onto an EPG electrode that was held at −20 mV and rotated at 100 rpm in air-saturated solutions of 20 mM NaAcO with no added AcOH for (a) 300 s and (b) 1080 s. Data acquired in N$_2$-purged (---) and air-saturated (—) solutions of 100 mM NaClO$_4$ at 100 mV/s.

phen) has the most positive $E_{cat.}^0$ of the complexes examined; it is 265 mV more positive than Cu(5-NO$_2$-phen) and 80 mV more positive than Cu(2,9-Me$_2$-phen).

The third more subtle trend is that increases in $E_{cat.}^0$ along either of the first two trends lead to increases in the difference between E_{O_2} and $E_{cat.}^0$. For example, the difference increases from 10 mV in Cu(5-Cl-phen) to 20 mV for Cu(3,8-(CO$_2$Et)$_2$-4,7-Cl$_2$-phen) and from 10 mV in Cu(2-Me-phen) to 80 mV for Cu(2,9-n-Bu$_2$-phen). The Cu complex with the highest reported $E_{cat.}^0$, Cu(2,9-Me$_2$-5-NO$_2$-phen), has a difference between E_{O_2} and $E_{cat.}^0$ of 310 mV.

Hydrodynamic Studies. A kinetic analysis of the electrocatalytic O_2 reduction by Cu phen-based complexes was conducted at rotating-disk electrodes. Rotating the electrode sweeps dissolved O_2 past the electrode, creating a steady-state concentration at the electrode surface. The resulting steady-state voltammograms for Cu(phen) and Cu(2,9-Me$_2$-phen) are presented in Figure 9a,b. At any potential E, as the electrode is rotated at increasing rotation rate, the steady-state current asymptotically approaches the kinetic current $i_K(E)$, which is the current at which mass transfer plays no role and the reaction is limited only by the kinetics at the electrode surface. This behavior follows the Koutecky−Levich equation:[24]

$$i(E)^{-1} = i_K(E)^{-1} + i_L^{-1} \qquad (1)$$

where $i(E)$ is the measured current, and i_L is the Levich current, given by[24]

$$i_L = -0.62nFA(D_{O_2})^{2/3}\omega^{1/2}\nu^{-1/6}[O_2] \qquad (2)$$

Here n is the number of electrons transferred, F is Faraday's constant, $A = 0.195$ cm^2 is the electrode macroscopic surface area, $D_{O_2} = 1.8 \times 10^{-5}$ cm^2 s^{-1} is the diffusion coefficient of O_2 in aqueous solutions,[25] ω is the angular rotation rate, $\nu =$
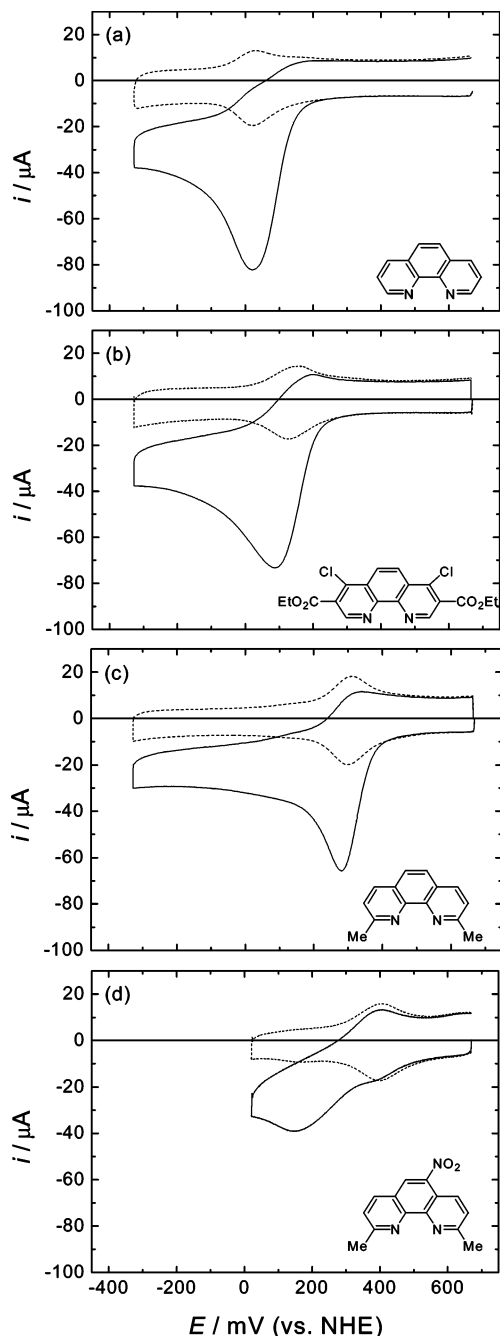
Electrocatalytic Reduction of O$_2$ to H$_2$O

J. Phys. Chem. A, Vol. 111, No. 49, 2007 **12645**

Figure 8. CVs of EPG surface-adsorbed Cu complexes of (a) phen, (b) 3,8-(CO$_2$Et)$_2$-4,7-Cl$_2$-phen, (c) 2,9-Me$_2$-phen, and (d) 2,9-Me$_2$-5-NO$_2$-phen, in N$_2$-purged (- - -) and air-saturated (—) solutions of 100 mM NaClO$_4$, 20 mM NaAcO, 20 mM AcOH, pH 4.8 at 100 mV/s.

0.009 cm^2 s^{-1} is the kinematic viscosity of the solution,[24] and [O$_2$] = 0.26 mM is the concentration of O$_2$ in air-saturated 100 mM NaClO$_4$ solutions.[26]

Plots of $i(E)^{-1}$, the inverse of the current measured at a constant potential E, as a function of $\omega^{-1/2}$ yield $i_K(E)^{-1}$ as the intercept,[24] as shown in Figure 9c,d at −150 mV vs NHE for phen and 2,9-Me$_2$-phen, respectively. The dashed lines are the inverse Levich currents calculated from eq 2 for 2 e$^-$ ($n = 2$) and 4 e$^-$ ($n = 4$) reductions of O$_2$. At potentials negative of $E_{cat.}^0$, the plots of the observed inverse currents are parallel to the inverse Levich currents calculated with $n = 4$, suggesting that the adsorbed complex catalyzes a 4 e$^-$, rather than a 2 e$^-$, reduction of O$_2$. As a control experiment, the kinetic current in air-saturated solution at a bare EPG electrode was measured and found to be less than 8% of the kinetic current in the

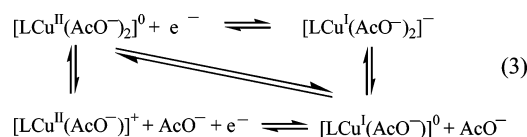presence of adsorbed catalyst. Therefore, we neglect the uncatalyzed reduction in our analysis.[27]

Kinetic analyses were conducted for a variety of Cu phen-based complexes. The $i_K(E)$ values were normalized by the catalyst redox charge, $q_{cat.}$, yielding a rate of electron delivery (in units of s^{-1}) free from mass-transfer effects. Plots of this normalized kinetic current, $i_K(E)/q_{cat.}$, as a function of potential are shown in Figure 10 for Cu(phen), Cu(3,8-(CO$_2$Et)$_2$-4,7-Cl$_2$-phen), Cu(2-Me-phen), and Cu(2,9-Me$_2$-phen). For all complexes, the value of $i_K(E)/q_{cat.}$ reaches less than half of its maximum value at $E_{cat.}^0$. Several of the normalized kinetic currents measured at $E_{cat.}^0$ are shown in the Table 1.

The normalized kinetic current measured at the very negative potential of −150 mV vs NHE, $i_K(-150\text{mV})/q_{cat.}$, decreases very gradually as the $E_{cat.}^0$ of the catalysts increases (Figure 11). The normalized kinetic current measured at $E_{cat.}^0$, $i_K(E_{cat.}^0)/q_{cat.}$, shows a more complex dependence. For instance, as $E_{cat.}^0$ increases due to the addition of electron-withdrawing substituents, $i_K(E_{cat.}^0)/q_{cat.}$ decreases rapidly. However, when $E_{cat.}^0$ increases due to the addition of progressively larger substituents adjacent to the Cu coordination site, $i_K(E_{cat.}^0)/q_{cat.}$ decreases more gradually. A clear example of this complicated dependence of $i_K(E_{cat.}^0)/q_{cat.}$ on the substituents is that $i_K(E_{cat.}^0)/q_{cat.}$ for Cu-(2-Me-phen) is 4 times *larger* than that for Cu(3,8-CO$_2$Et-4,7-Cl$_2$-phen), even though $E_{cat.}^0$ for Cu(2-Me-phen) is 75 mV *more positive* than that of Cu(3,8-CO$_2$Et-4,7-Cl$_2$-phen).

To ensure that the observed kinetic current $i_K(E)$ is first order in O$_2$, the Cu(phen) catalyst was investigated at different [O$_2$]. The kinetic currents, normalized for [O$_2$] and $q_{cat.}$, are shown as squares and circles in Figure 12 for [O$_2$] = 0.26 mM and [O$_2$] = 0.12 mM, respectively. These normalized currents overlay at all potentials, as expected for a first-order dependence in O$_2$. In addition, to ensure that the observed kinetic currents are independent of AcOH and electrolyte concentrations, each were varied (Figure 12). Again, the kinetic currents normalized for [O$_2$] and $q_{cat.}$ overlay at all potentials for values of [AcOH] > 2 mM and both values of [NaClO$_4$] explored.[28]
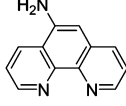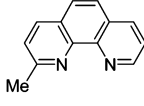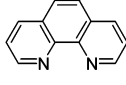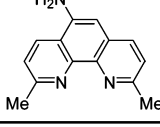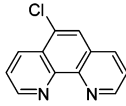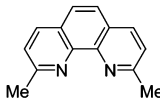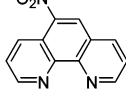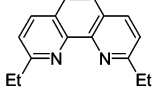
Discussion

Anion Effects. The ca. 60 mV/decade shift in $E_{cat.}^0$ with increasing [AcO$^-$] (Figures 2 and 3) is a Nernstian behavior, indicating that the reduction of Cu^{II} to Cu^I is accompanied by a dissociation of a coordinating anion. We propose the following square scheme for the reduction/oxidation and the dissociation/association reactions:

$$[\text{LCu}^{II}(\text{AcO}^-)_2]^0 + e^- \rightleftharpoons [\text{LCu}^I(\text{AcO}^-)_2]^-$$
$$\quad (3)$$
$$[\text{LCu}^{II}(\text{AcO}^-)]^+ + \text{AcO}^- + e^- \rightleftharpoons [\text{LCu}^I(\text{AcO}^-)]^0 + \text{AcO}^-$$

As prepared, the phen-based ligand L adsorbs into the EPG, most likely diffusing into the crevices that characterize the electrode's su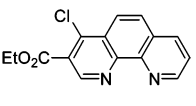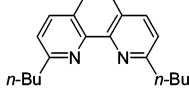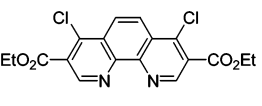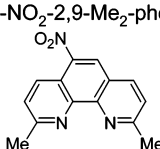rface (Figure 1). Subsequent exposure to Cu-(NO$_3$)$_2$(aq) presumably forms a LCu^{II} species. Exposure of the electrode to solutions of coordinating anions (such as AcO$^-$, HCO$_3^-$, and CO$_3^-$) can lead to the formation of many species given the extreme lability of Cu$^{II/I}$. For simplicity, we will consider only coordinating AcO$^-$ and assume that we start from LCu^{II}(AcO$^-$)$_2$. Reduction of LCu^{II}(AcO$^-$)$_2$ yields [LCu^I(AcO$^-$)$_2$]$^-$. This is in equilibrium with LCu^I(AcO$^-$), the one-electron reduction product of [LCu^{II}(AcO$^-$)]$^+$. The observed shift in $E_{cat.}^0$ of −60 mV/decade of [AcO$^-$] (Figure 3) is consistent

TABLE 1: Ligands Adsorbed onto EPG and Complexed with Cu^{II} [a]

e⁻ Donating / Withdrawing Substituents Remote to Cu-Binding Site	E^0_{cat} mV vs. NHE	E_{O_2} mV vs. NHE	$\dfrac{i_K(E^0_{cat})}{q_{cat}}$ s⁻¹	Substituents Adjacent to Cu-Binding Site	E^0_{cat} mV vs. NHE	E_{O_2} mV vs. NHE	$\dfrac{i_K(E^0_{cat})}{q_{cat}}$ s⁻¹
5-NH₂-phen	20	*10*	—	2-Me-phen	215	*205*	**7 ± 2**
phen	25	*10*	**16 ± 3**	5-NH₂-2,9-Me₂-phen	285	*275*	—
5-Cl-phen	50	*40*	—	2,9-Me₂-phen	310	*290*	**1.6 ± 0.5**
5-NO₂-phen	75	*40*	—	2,9-Et₂-phen	335	*305*	**0.4 ± 0.2**
3-CO₂Et-4-Cl-phen	90	*65*	**6 ± 2**	2,9-nBu₂-phen	340	*260*	—
3,8-(CO₂Et)₂-4,7-Cl₂-phen	150	*130*	**1.9 ± 0.5**	5-NO₂-2,9-Me₂-phen	390	*80*	—

[a] The first value reported is the potential of the Cu$^{II/I}$ redox couple, E^0_{cat}. The second value corresponds to the potential of the electrocatalytic O₂-reduction peak, E_{O_2} (scan rate = 100 mV/s). The third value corresponds to the normalized kinetic current for O₂ reduction at E^0_{cat}. All data taken in aqueous solutions of 100 mM NaClO₄, 20 mM NaAcO, 20 mM AcOH, pH 4.8.

with the net reaction from LCu^{II}(AcO⁻)₂ to LCu^{I}(AcO⁻), shown as the diagonal in eq 3.

At low [AcO⁻], some Cu species are electroinactive (Figures 2 and 4). We propose that upon binding of positively charged Cu to the adsorbed neutral ligands, a positive space-charge layer is formed at or in the graphite surface. This space charge is only neutralized by the coordination of AcO⁻ to the adsorbed Cu complexes. At low [AcO⁻], the positive space-charge layer facilitates the reduction of the most deeply coordinated Cu species. This shifts their redox potentials positive of the accessible potential window for graphite electrodes in aqueous solutions, thus making them electrochemically inaccessible.

Increasing [AcO⁻] drives the coordination of AcO⁻ (eq 3), neutralizing the space-charge layer and shifting more of the deeply coordinated Cu species into the accessible potential range. This increases the amount of electroactive Cu, as seen in Figure 4. With sufficient [AcO⁻], the space-charge layer should be eliminated and all Cu species should be electroactive

with a single standard redox potential and a full-width-at-half-maximum approaching the theoretical value of 90 mV.[29] A relatively narrow redox peak of width 120 mV is indeed observed at high [AcO⁻] (Figure 2).

The fact that the measured $q_{cat.}$ at high [AcO⁻] corresponds to only 30% of the deposited phen ligand suggests that the space-charge layer formed during exposure to Cu(NO₃)₂(aq) inhibits binding of Cu in the most deeply adsorbed phen ligands. This suggests that exposing the electrode to aqueous solutions of Cu(NO₃)₂ and some coordinating anion to neutralize the space charge should increase the measured $q_{cat.}$. This is observed in the ca. 150% increase in the measured charge for electrodes exposed to solutions of 0.5 M Cu(NO₃)₂ and 1 M NaAcO when compared with electrodes exposed to solutions of 0.5 M Cu(NO₃)₂ and 10 mM NaAcO.

Ligand Effects on $E_{cat.}^0$ and E_{O_2}. $E_{cat.}^0$ and E_{O_2} of the Cu complexes were varied by altering the substituents on the phen

Electrocatalytic Reduction of O₂ to H₂O

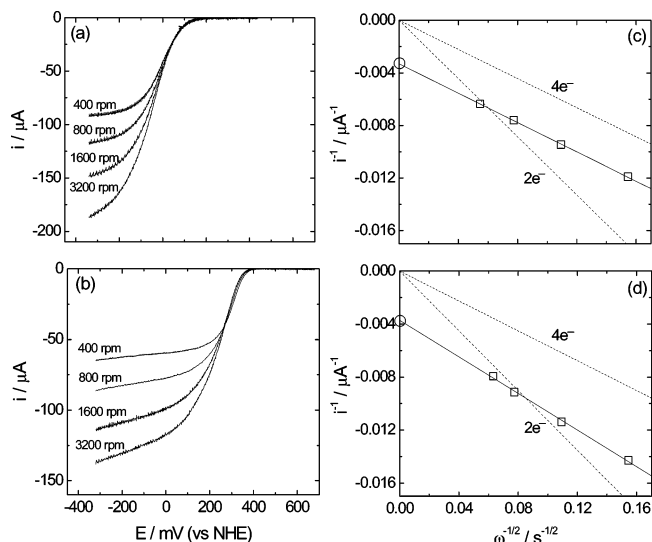*J. Phys. Chem. A, Vol. 111, No. 49, 2007* **12647**

Figure 9. Current vs potential curves for the reduction of 0.28 mM O₂ catalyzed by (a) Cu(phen) and (b) Cu(2,9-Me₂-phen) on a rotating EPG electrode (100 mM NaClO₄; 20 mM NaAcO; 20 mM AcOH; pH 4.8; 25 mV/s). Koutecky−Levich plots of the inverse of the plateau current of (a) and (b) measured at −150 mV as a function of the (rotation rate)$^{-1/2}$ are shown in (c) and (d). The dashed lines give the calculated responses for a diffusion-controlled reduction of O₂ by 2 and 4 electrons. The fitted lines yield (c) $n = 4.0 \pm 0.1$ and (d) $n = 3.4 \pm 0.2$. The circled intercept is the inverse of the kinetically limited current, i_K.
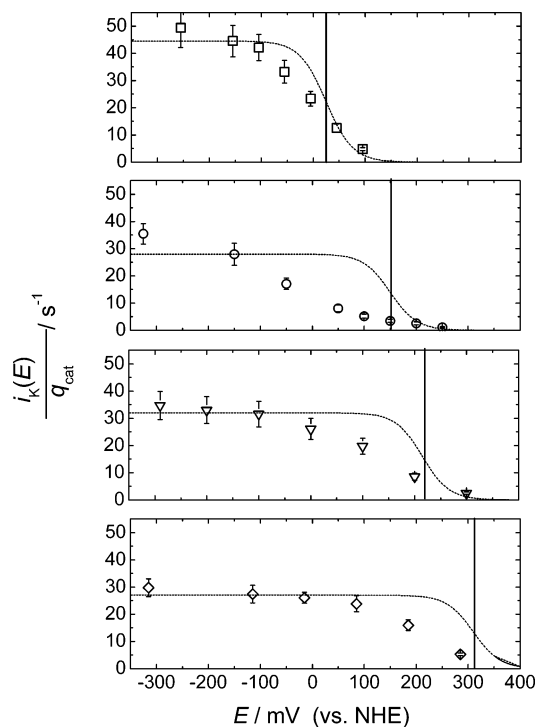

Figure 10. Normalized kinetic currents at for Cu complexes of phen (squares); 3,8-(CO₂Et)₂-4,7-Cl₂-phen (circles); 2-Me-phen (triangles); 2,9-Me₂-phen (diamonds), in air-saturated solutions (100 mM NaClO₄, 20 mM NaAcO, 20 mM AcOH, pH 4.8 for phen and 3,8-(CO₂Et)₂-4,7-Cl₂-phen; 100 mM NaClO₄, 20 mM NaAcO and 72 mM AcOH, pH 4.2 for 2,9-Me₂-phen. The vertical solid lines are $E^0_{cat.}$ for the given catalyst. The dashed lines are the expected responses if O₂ binding were rate limiting at all potentials.

ligands. For substituents that are not adjacent to the Cu-binding site (Table 1, columns 1−3), more electron-donating ligands, for instance 5-NH₂-phen, shift $E^0_{cat.}$ and E_{O_2} to more negative potentials. This implies that electron-donating ligands prefer-
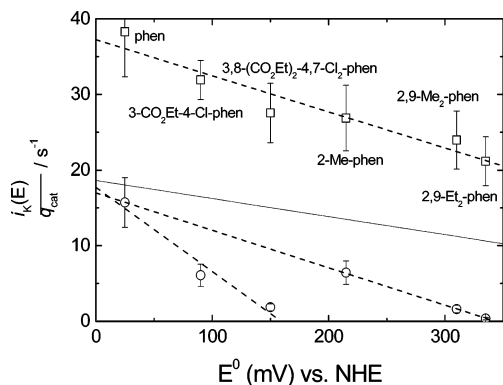

Figure 11. Normalized kinetic currents for Cu complexes measured at $E^0_{cat.}$ (circles) and at −150 mV vs NHE (squares) are plotted against $E^0_{cat.}$ for each Cu complex. A single functional form of the decrease in the normalized kinetic current with increasing $E^0_{cat.}$ is not obvious, and linear fits (dashed lines) are proposed as guides to the eye for proposed trends. The dotted line is the expected behavior for the kinetic current measured at $E_{1/2}$. All data taken in 20 mM NaAcO and 20 mM AcOH pH 4.8, 100 mM NaClO₄ except 2,9-Me₂-phen taken in 20 mM NaAcO and 72 mM AcOH pH 4.2, 100 mM NaClO₄.
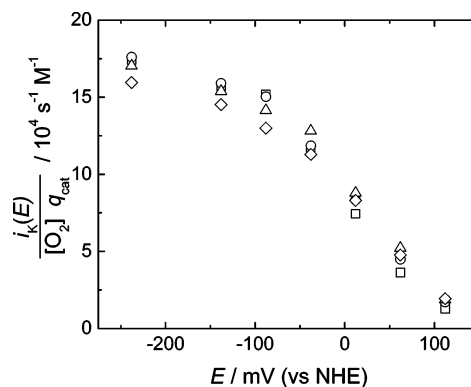

Figure 12. Kinetic rates at different potentials normalized for $q_{cat.}$ and [O₂] for Cu(phen) in (squares) 6.133 mM AcOH, 20 mM NaAcO, 100 mM NaClO₄, air-saturated (0.26 mM [O₂]); (circles) 12.26 mM AcOH, 20 mM NaAcO, 100 mM NaClO₄, air-saturated (0.26 mM [O₂]); (triangles) 12.26 mM AcOH, 20 mM NaAcO, 100 mM NaClO₄, saturated with 10% O₂ (0.12 mM [O₂]); (diamonds) 12.26 mM AcOH, 20 mM NaAcO, 550 mM NaClO₄, air-saturated (calculated at 0.23 mM [O₂]).

entially stabilize the Cu^{II} oxidation state. Ligands with electron-withdrawing substituents have the opposite effect. The range of these shifts is ca. 130 mV.

The effects of 2,9 substituents on the phen ligand, adjacent to the Cu-binding site, cannot be explained by electronic effects. Instead we find that increasing the size of the substituents in these positions shifts $E^0_{cat.}$ and E_{O_2} positive (Table 1, columns 5−7) up to 300 mV. We postulate that these 2,9 substituents destabilize the Cu^{II} oxidation state by distorting the energetically preferred square-planar coordination around the Cu^{II}. The geometry of the Cu^{I} complex is presumably either 3-coordinate or tetrahedral 4-coordinate, which are accommodated readily even with sterically demanding substituents on the phen ligands (Figure 13). The steric demands at the 2,9 positions and the electronic effects at other positions can be combined, as in the case of 5-NO₂-2,9-Me₂-phen, for which $E^0_{cat.}$ is 80 mV more positive than that for 2,9-Me₂-phen, and in the case of 5-NH₂-2,9-Me₂-phen, for which $E^0_{cat.}$ is 25 mV more negative than that for 2,9-Me₂-phen.

O₂-Reduction Kinetics. A suggested mechanism for the electrocatalytic reduction of O₂ by Cu phen-based catalysts is
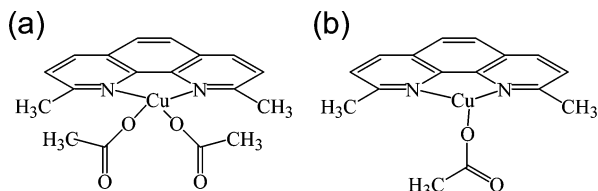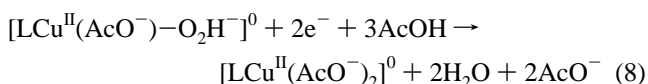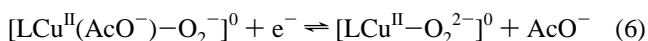
(a)   (b)

Figure 13. Proposed structure for (a) $[Cu^{II}(2,9\text{-}Me_2\text{-phen})(AcO^-)_2]^0$ and (b) $[Cu^I(2,9\text{-}Me_2\text{-phen})(AcO^-)]^0$. The steric demands of the 2,9 methyl substituents impact the Cu coordination much more in (a) the square-planar Cu(II) complex than (b) the trigonally ligated Cu(I) complex.
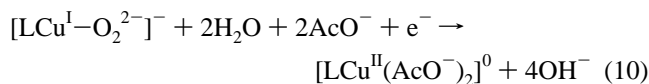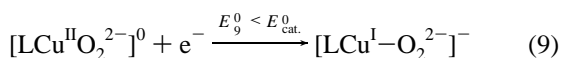
presented in eqs 4−8. This mechanism expands upon that proposed by Lei and Anson by providing for additional rate-limiting steps:[7]

$$[LCu^{II}(AcO^-)_2]^0 + e^- \underset{}{\overset{E^0_{cat.}}{\rightleftharpoons}} [LCu^I(AcO^-)]^0 + AcO^- \quad (4)$$

$$[LCu^I(AcO^-)]^0 + O_2 \underset{}{\overset{k_{O_2}}{\rightleftharpoons}} [LCu^{II}(AcO^-)-O_2^-]^0 \quad (5)$$

$$[LCu^{II}(AcO^-)-O_2^-]^0 + e^- \rightleftharpoons [LCu^{II}-O_2^{2-}]^0 + AcO^- \quad (6)$$

$$[LCu^{II}-O_2^{2-}]^0 + AcOH \rightleftharpoons [LCu^{II}(AcO^-)-O_2H^-]^0 \quad (7)$$

$$[LCu^{II}(AcO^-)-O_2H^-]^0 + 2e^- + 3AcOH \rightarrow$$
$$[LCu^{II}(AcO^-)_2]^0 + 2H_2O + 2AcO^- \quad (8)$$

The reduction of O_2 negative of $E^0_{cat.}$ strongly suggests that the first step must be the reduction of Cu^{II} to Cu^I. The binding of O_2 likely results in the formation of Cu^{II}−superoxide intermediate (eq 5), which has been seen spectroscopically and structurally characterized for other mononuclear Cu centers with multidentate nitrogen-based ligands,[1,30−32] and is proposed for a variety of mononuclear Cu monoxygenases.[33] Because this step involves an electron transfer from a Cu^I to O_2 upon O_2-binding, the rate of this step might be dependent on $E^0_{cat.}$. The superoxide complex is presumed to be reduced prior to protonation because protonated superoxide coordinated to the Cu complex should be a significantly stronger acid than protonated superoxide in aqueous solution, for which the pK_a is 4.8.[34] Reduction of this Cu^{II}−superoxide complex results in the formation of a Cu^{II}−peroxide species (eq 6), which is then protonated in the presence of AcOH (eq 7), followed by rapid reduction and protonation to release water in an indeterminate number of steps (eq 8).

Although eqs 4−7 propose O_2 reduction through single electron transfers to superoxide and peroxide intermediates, this is not to suggest that these intermediates are formed in isolation through an outer-sphere mechanism at the electrode surface. The outer-sphere single electron reduction of O_2 to HO_2 at pH 4.8 is expected at $E^0 = -423$ mV vs NHE.[34] The rate of such an outer-sphere reduction would be expected to be negligible at the E_{O_2} values reported in Table 1. Instead, O_2 is reduced within the bonding radius of Cu, allowing stabilization of the partially reduced O_2 intermediates through coordination with the metal center. The formal charges on O_2 and Cu and the labels "superoxide" and "peroxide" are only used for book-keeping.

In the absence of AcOH, we propose a branch in the mechanism after eq 6:

$$[LCu^{II}O_2^{2-}]^0 + e^- \xrightarrow{E^0_9 < E^0_{cat.}} [LCu^I-O_2^{2-}]^- \quad (9)$$

$$[LCu^I-O_2^{2-}]^- + 2H_2O + 2AcO^- + e^- \rightarrow$$
$$[LCu^{II}(AcO^-)_2]^0 + 4OH^- \quad (10)$$

Without sufficient [AcOH], there is presumably no protonation of the Cu^{II}−peroxide product from eq 6. This Cu^{II}−peroxide species is presumed to react slowly with the ligand causing the observed irreversible changes in Figure 7. Reduction of the Cu^{II}−peroxide complex is expected to occur at more negative potential (eq 9) than the reduction of $[LCu^{II}(AcO^-)-O_2H^-]^0$ formed in the presence of AcOH (eq 8). For instance, in the case of $Cu(2,9\text{-}Me_2\text{-phen})$ measured in air-saturated solutions without added AcOH, the O_2-reduction peak is ca. 150 mV negative of $E^0_{cat.}$ (Figure 6a). This reduction is presumably followed by rapid protonation by H_2O and further reduction in an indeterminate number of steps. (eq 10).

At high [AcOH] and at very negative potential, the e^--transfer and H^+-transfer steps will be fast, so the rate-limiting step for the reaction will be eq 5 (the rate-limiting step proposed by Anson and co-workers).[7] In this case, the kinetically limited current i_K depends only on the kinetics of O_2 binding and is given by

$$i_K(E) = nFAk_{O_2}\Gamma_{cat}(E)[O_2] \quad (11)$$

Here k_{O_2} is the rate constant for O_2 binding, and $\Gamma_{cat}(E)$ is the coverage of reduced catalyst at a given potential. If O_2 binding were rate limiting at all potentials, the potential dependence of the kinetic current i_K would be a steady-state Nernstian $i-E$ curve with $i_K(E)$ equal to half its maximum value at $E^0_{cat.}$ (see Supporting Information). This is shown as the set of dashed curves in Figure 10. Although this model is somewhat consistent with the measured normalized kinetic currents in the case of Cu(phen), the normalized kinetic currents in the cases of Cu-$(3,8\text{-}(CO_2Et)_2\text{-}4,7\text{-}Cl_2\text{-phen})$, Cu(2-Me-phen), and Cu(2,9-Me_2-phen) diverge significantly from this Nernstian model near $E^0_{cat.}$. This divergence is shown further in Figure 11, in which the dotted line is the expected value from eq 11 of the normalized kinetic current at $E^0_{cat.}$. Note that all complexes have measured normalized kinetic currents at $E^0_{cat.}$ lower than this value. The differences between the experimental data and the model suggest that some potential-dependent step other than O_2-binding plays a rate-limiting role in the mechanism.

Because Cu^I is required for O_2 binding, the other rate-limiting reaction may be the initial reversible reduction of Cu^{II} to Cu^I (eq 4). The standard rate constant of the $Cu^{II/I}$ couple can be estimated from the separation of the Cu^{II}-reduction and Cu^I-oxidation peaks in N_2-purged electrolyte using an analysis due to Laviron.[35] As shown in the Supporting Information, the measured kinetics of this step do not account for the full magnitude of the suppression of the kinetic current near $E^0_{cat.}$, especially in the cases of $Cu(2,9\text{-}Me_2\text{-phen})$ or $Cu(3,8\text{-}(CO_2\text{-}Et)_2\text{-}4,7\text{-}Cl_2\text{-phen})$. We conclude that the initial reduction of Cu^{II} to Cu^I is not the only rate-limiting step near $E^0_{cat.}$ and suggest that one of the subsequent reductions of the partially reduced O_2 species coordinated to Cu is also rate limiting. One possibility is that the reduction of the superoxide complex to the peroxide complex, which has a fairly negative standard redox potential, is less dependent on the specific phen-based ligand used than is the Cu^{II} to Cu^I reduction at $E^0_{cat.}$. As variations in the phen-based ligand shift $E^0_{cat.}$ more positive, reduction of the super-oxide near $E^0_{cat.}$ would then be more energetically uphill and thus become slower. At values of $E^0_{cat.}$ more positive than $+350$ mV vs NHE, the reduction of the superoxide would be

too unfavorable to occur at a significant rate, and so electro-catalytic O_2 reduction would not be observed.

Kinetic Limits with Mononuclear Cu Complexes. As the $E_{cat.}^0$ of the catalysts increase, a corresponding decrease in the rate of O_2 reduction is observed. This is true of both the magnitude of the normalized kinetic currents at a very negative potential and those at the standard potential of the catalyst (Figure 11). However, the values at very negative potential, which are presumably limited only by O_2 binding, decrease very gradually as the $E_{cat.}^0$ of the catalysts increases: from 38 ± 6 s^{-1} for Cu(phen) to 21 ± 3 s^{-1} for Cu(2,9-Et$_2$-phen). This decrease in rate is presumably due to a decrease in the stabilization of the superoxide intermediate by the Cu center (eq 5). Regardless, the slope of the decrease is shallow, suggesting that O_2 binding is not a severe limitation even for catalysts with very positive standard potentials.

On the other hand, the magnitude of the normalized kinetic currents at the standard potential of the catalyst $E_{cat.}^0$ decreases more rapidly as $E_{cat.}^0$ of the catalyst increases: from 16 ± 3 s^{-1} for Cu(phen) to 1.9 ± 0.5 s^{-1} for the electron-withdrawing Cu-(3,8-(CO$_2$Et$_2$)-4,7-Cl$_2$-phen) and 0.4 ± 0.2 s^{-1} for the sterically demanding Cu(2,9-Et$_2$-phen). In the case of increasing steric demands at the Cu binding site, a simple linear extrapolation of the normalized kinetic current measured at the standard potential of the catalyst predicts no O_2 reduction for complexes with standard potentials greater than ca. $+350$ mV vs NHE. This is an overpotential of -590 mV with respect to the reversible O_2-reduction potential at this pH. The trend falls off even more rapidly for complexes with increasing electron-withdrawing substituents. We therefore believe it is unlikely that any mononuclear Cu complex will catalyze the electrore-duction of O_2 at more positive potentials than ca. $+350$ mV vs NHE.

Conclusions

The effects of [AcO$^-$] and [AcOH] on the electrocatalytic reduction of O_2 by phenanthroline complexes of Cu were investigated. The reduction from Cu^{II} to Cu^I is accompanied by the dissociation of an AcO$^-$ or other coordinating anion. It was also shown that for O_2 reduction to occur near $E_{cat.}^0$, it is necessary for a specific acid, in this case acetic acid, to be present in reasonable quantities. Irreversible degradation of the catalyst occurs if O_2 reduction is performed in the absence of acetic acid. We propose that the Cu^{II}-peroxide species has a longer lifetime because it only decays by an unfavorable reduction and can presumably attack the ligand substituents in the mean time. The contributions of the first two rate-limiting steps in the proposed electrocatalytic mechanism of O_2 reduction to H_2O were investigated: the initial reduction of Cu^{II} to Cu^I and O_2 binding to Cu^I. At least one of the latter reduction steps after eq 5 must be rate limiting to account for the low measured currents at $E_{cat.}^0$.

The ligand effects on the electrocatalytic potentials and currents were also investigated. In particular, the $E_{cat.}^0$ of Cu complexes of phen-based ligands was driven positive by addition of electron-withdrawing groups on the ligand and by increasing the steric demands near the Cu center by adding groups to the 2 and 9 positions on the phen. However, the rate of O_2 reduction decreases with increasing $E_{cat.}^0$. Specifically, the rate measured at $E_{cat.}^0$ appears to decrease linearly with increasing $E_{cat.}^0$ according to two distinct trends—one follows the electron-withdrawing capacity of the ligand; the other, the size of the substituents in the 2 and 9 positions.

An extrapolation of these trends suggests that normalized kinetic currents of 1 s^{-1} are expected at ca. 335 mV vs NHE. This corresponds to a reduction rate of 0.25 O_2 per Cu s^{-1} at an overpotential of -605 mV from the thermodynamic potential of O_2 reduction. Pt nanoparticulate catalysts operate at the same rate and at more favorable overpotentials of -350 mV. No electrocatalytic activity is predicted for mononuclear molecular Cu complexes with $E_{cat.}^0$ more positive than $+350$ mV vs NHE. However, it is clear that multinuclear Cu complexes such as fungal laccase can be effective catalysts at much more positive potentials. We suggest that using multinuclear Cu complexes in which two or more metal centers are situated such that they can interact with O_2 simultaneously are needed to efficiently catalyze the reduction of O_2 at more positive $E_{cat.}^0$. We intend to explore synthetic multinuclear complexes of Cu to determine the minimal coordination environment needed for effective catalysis at more positive potentials.

Supporting Information Available: Scan-rate dependence analysis, derivations of the kinetic models used in the data analysis, and a summary of other ligands investigated in this study. This material is available free of charge via the Internet at http://pubs.acs.org.

References and Notes

(1) Mirica, L. M.; Ottenwaelder, X.; Stack, T. D. P. *Chem. Rev.* **2004**, *104*, 1013−1045.

(2) Solomon, E. I.; Sundaram, U. M.; Machonkin, T. E. *Chem. Rev.* **1996**, *96*, 2563−2605.

(3) Barton, S. C.; Kim, H. H.; Binyamin, G.; Zhang, Y. C.; Heller, A. *J. Am. Chem. Soc.* **2001**, *123*, 5802−5803.

(4) Barton, S. C.; Kim, H. H.; Binyamin, G.; Zhang, Y. C.; Heller, A. *J. Phys. Chem. B* **2001**, *105*, 11917−11921.

(5) Soukharev, V.; Mano, N.; Heller, A. *J. Am. Chem. Soc.* **2004**, *126*, 8368−8369.

(6) Ralph, T. R.; Hogarth, M. P. *Platinum Met. Rev.* **2002**, *46*, 3−14.

(7) Lei, Y.; Anson, F. C. *Inorg. Chem.* **1994**, *33*, 5003−5009.

(8) Lei, Y.; Anson, F. C. *Inorg. Chem.* **1995**, *34*, 1083−1089.

(9) Zhang, J.; Anson, F. C. *J. Electroanal. Chem.* **1992**, *341*, 323−341.

(10) Zhang, J.; Anson, F. C. *Electrochim. Acta* **1993**, *38*, 2423−2429.

(11) Rorabacher, D. B. *Chem. Rev.* **2004**, *104*, 651−697.

(12) Poole, R. A.; Bobba, G.; Cann, M. J.; Frias, J. C.; Parker, D.; Peacock, R. D. *Org. Biomol. Chem.* **2005**, *3*, 1013−1024.

(13) Garcia-Fresnadillo, D.; Orellana, G. *Helv. Chim. Acta* **2001**, *84*, 2708−2730.

(14) Astrom, H.; Stromberg, R. *Org. Biomol. Chem.* **2004**, *2*, 1901−1907.

(15) Vannelli, T. A.; Karpishin, T. B. *Inorg. Chem.* **2000**, *39*, 340−347.

(16) Pallenberg, A. J.; Koenig, K. S.; Barnhart, D. M. *Inorg. Chem.* **1995**, *34*, 2833−2840.

(17) Markees, D. G. *Helv. Chim. Acta* **1983**, *66*, 620−626.

(18) Molock, F. F.; Boykin, D. W. *J. Heterocycl. Chem.* **1983**, *20*, 681−686.

(19) Snyder, H. R.; Freier, H. E. *J. Am. Chem. Soc.* **1946**, *68*, 1320−1322.

(20) Putnam, W. C.; Daniher, A. T.; Trawick, B. N.; Bashkin, J. K. *Nucleic Acids Res.* **2001**, *29*, 2199−2204.

(21) Bard, A. J.; Faulkner, L. R. *Electrochemical Methods: Fundamentals and Applications*, 2nd ed.; John Wiley & Sons, Inc.: New York, 2001; pp 810.

(22) The CV was baseline corrected by subtraction of a background CV obtained with uncomplexed 2,9-Me$_2$-phen adsorbed onto an EPG electrode. Manually setting a baseline by visual inspection yielded similar results.

(23) A constant rate of O$_2$ delivery to the electrode was achieved by rotating the electrode at 100 rpm. This is explored in more detail later to quantify kinetic currents.

(24) Bard, A. J.; Faulkner, L. R. *Electrochemical Methods: Fundamentals and Applications*, 2nd ed.; John Wiley & Sons, Inc.: New York, 2001; pp 335−344.

(25) Chang, P.; Wilke, C. R. *J. Phys. Chem.* **1955**, *59*, 592−600.

(26) Battino, R.; Rettich, T. R.; Tominaga, T. *J. Phys. Chem. Ref. Data* **1983**, *12*, 163−78.

(27) The kinetic current due to O$_2$ reduction to H$_2$O$_2$ at −150 mV vs NHE at a 0.195 cm^2 electrode in a standard pH 4.8, 20 mM AcO$^-$/20 mM AcOH buffer solution was determined from a Koutecky−Levich analysis to be −26 μA. Upon adsorption of ca. 5 × 10^{-10} mol/cm^2 of Cu(phen) to the same electrode, the resulting kinetic current due to O$_2$ reduction to H$_2$O was determined to be −347 μA, so the kinetic current due to O$_2$ reduction to H$_2$O$_2$ was ca. 8%. Similarly, Anson and colleagues reported less than

6% peroxide generation at -60 mV vs. NHE and fast rotations rates at EPG electrodes with adsorbed Cu(phen) (ref 8).

(28) [O$_2$] in air-saturated 0.55 M NaClO$_4$ was calculated to be 0.23 mM from reported solubility parameters (Battino, R.; Rettich, T. R.; Tominaga, T. J.; *Phys. Chem. Ref. Data* **1983**, *12*, 163−178.)

(29) Bard, A. J.; Faulkner, L. R. *Electrochemical Methods: Fundamentals and Applications*, 2nd ed.; John Wiley & Sons, Inc.: New York, 2001; pp 589−593.

(30) Aboelella, N. W.; Lewis, E. A.; Reynolds, A. M.; Brennessel, W. W.; Cramer, C. J.; Tolman, W. B. *J. Am. Chem. Soc.* **2002**, *124*, 10660−10661.

(31) Fujisawa, K.; Tanaka, M.; Morooka, Y.; Kitajima, N. *J. Am. Chem. Soc.* **1994**, *116*, 12079−12080.

(32) Schatz, M.; Raab, V.; Foxon, S. P.; Brehm, G.; Schneider, S.; Reiher, M.; Holthausen, M. C.; Sundermeyer, J.; Schindler, S. *Angew. Chem. Int. Ed.* **2004**, *43*, 4360−4363.

(33) Itoh, S. *Curr. Opin. Chem. Biol.* **2006**, *10*, 115−122.

(34) Hoare, J. P. Oxygen. In *Standard Potentials in Aqueous Solution*; Bard, A. J., Parsons, R., Jordan, J., Eds.; Marcel Dekker, Inc.: New York 1985; pp 49−66.

(35) Laviron, E. *J. Electroanal. Chem.* **1979**, *101*, 19−28.